

# Fabrication of Superhydrophobic Structure on 5A05 Aluminum Alloy Surface and Its Corrosion Resistance

Zhang Chuanwei<sup>1</sup>, Li Xuewu<sup>1</sup>, Shi Tian<sup>1</sup>, Zhang Laichang<sup>2</sup>

<sup>1</sup> Xi'an University of Science and Technology, Xi'an 710054, China; <sup>2</sup> Edith Cowan University, Perth 6027, Australia

**Abstract:** This work developed a simple and low-cost method to achieve superior superhydrophobicity and corrosion resistance of 5A05 Al alloy. The microscale wrinkles covered with nanoscale craters were prepared by a one-step wire electrical discharge machining process. Meanwhile, the wettability and corrosion resistance of the as-prepared structures were investigated after the low-surface-energy modification. The results show that the modified surface exhibits excellent superhydrophobicity with a water contact angle (CA) of 152.7° and a rolling angle (RA) of 7.1°. Furthermore, its corrosion resistance was assessed by electrochemical tests. Ultimately, owing to the trapped air in micro-nano structures, the solid-air-liquid interface helps to resist seawater penetration on the superhydrophobic surface and significantly enhances its corrosion resistance.

**Key words:** Al alloy; micro-nano structure; superhydrophobicity; corrosion resistance

Al alloys have attracted extensive interest due to their excellent behaviors, such as easy accessibility, good workability, high specific strength and low price<sup>[1]</sup>. Particularly, Al alloys are considered to be irreplaceable engineering plates, welding components and structural parts in ship building and marine fields<sup>[2]</sup>. Generally, thin oxide layers are easily formed on the Al alloy surfaces. However, such layers are prone to corrosion in marine and drippy conditions, leading to metal failures. Thereby their service life and application fields are severely restricted. Hence, it is of great economic value and practical significance to protect Al alloys from corrosion in seawater.

Various methods such as protective coating<sup>[3]</sup>, corrosion inhibitor<sup>[4]</sup>, alloying process<sup>[5]</sup>, laser treatment<sup>[6]</sup> and plating technology<sup>[7]</sup> have been developed to improve corrosion resistance of Al alloys. However, some coating techniques with heavy metal ions are contaminative. Laser treatment is usually uncontrollable. Some other methods may be costly and complicated. Therefore, the development of a simple, green and low-cost anticorrosion method for Al alloys remains a huge challenge.

Inspired by the self-cleaning and water-repelling behaviors

of lotus leaves<sup>[8]</sup>, fabricating superhydrophobic Al alloy surfaces can impede contact with the corrosive media, thereby slowing down their corrosion rates. As such, preparing superhydrophobic surfaces is a promising anticorrosion method. Generally, a superhydrophobic surface with a water contact angle (CA) larger than 150° and a rolling angle (RA) less than 10° is obtained by preparing micro-nano structures and low-surface-energy coatings. Up to now, various methods have been developed to prepare superhydrophobic Al alloys, such as anodizing process<sup>[9]</sup>, sol-gel process<sup>[10]</sup>, chemical etch<sup>[11]</sup>, boiling treatment<sup>[12]</sup>, galvanic replacement reactions<sup>[13]</sup> and immersing process<sup>[14]</sup>. Besides, Zhang et al<sup>[15]</sup> have fabricated a superhydrophobic 2024 Al alloy coating by chemical vapor deposition and surface modification. Xia et al<sup>[16]</sup> have fabricated a superhydrophobic Al-Mg metal by preparing amorphous tungsten oxide coatings and PFDTs-17 modification. Liu et al<sup>[17]</sup> have prepared a superhydrophobic 7075 Al alloy with good water repelling behavior through laser processing and anodic oxidization. However, the anticorrosion behaviors in seawater are seldom mentioned in above works. Meanwhile, the chemical stability is rarely investigated, which significantly restrains their practical

Received date: March 26, 2018

Foundation item: National Natural Science Foundation of China (51705416)

Corresponding author: Li Xuewu, Ph. D., Associate Professor, School of Mechanical Engineering, Xi'an University of Science and Technology, Xi'an 710054, P. R. China, Tel: 0086-29-83856323, E-mail: lixuewu55@xust.edu.cn

Copyright © 2018, Northwest Institute for Nonferrous Metal Research. Published by Elsevier BV. All rights reserved.

applications. In addition, the superhydrophobic surfaces can only be prepared under severe conditions by many of the aforementioned methods. Based on such analyses, developing a facile method to fabricate superhydrophobic Al alloys with enhanced corrosion resistance and chemical stability is of great practical significance.

In this work, a superhydrophobic 5A05 Al alloy with enhanced corrosion resistance in seawater was fabricated using a simple and low-cost wire electrical discharge machining (WEDM) and modification process. The WEDM process can produce micro-nano structures by controlling its electric pulse parameters. After the rough structures was silanized, a superhydrophobic surface with excellent adhesion resistance was obtained. Afterwards, the anticorrosion behaviors in seawater were assessed using electrochemical tests. These efforts provide positive insights for expanding the application of Al alloys as engineering materials in industrial fields.

## 1 Experiment

### 1.1 Materials

The commercially available 5A05 Al alloy plate was used. Its chemical composition is listed in Table 1. 1H, 2H, 2H-perfluorodecyltrichlorosilane modifier (PFDTs) was purchased from Tokyo Chemical Industry Co., Ltd, Japan. Other reagents were of analytical grade and obtained from Sinopharm Chemical Reagent Co., Ltd, China.

### 1.2 Preparation

A WEDM system (DK7732C type) was used with the one-way direct current pulse power. The as-prepared sample was used as the anode and the molybdenum wire electrode with a diameter of 80  $\mu\text{m}$  was used as the cathode. Firstly, the Al alloy plate was polished with metallographic abrasive paper and cut into specimens with a unified size of 10 mm  $\times$  10 mm  $\times$  5 mm. In the WEDM process, the power tube number, pulse interval, pulse width and frequency were set as 6, 50  $\mu\text{s}$ , 30  $\mu\text{s}$  and 40 Hz, respectively. Then, the specimens were ultrasonically cleaned in kerosene, acetone, ethanol and deionized water for 20 min. After drying with high purity nitrogen, surface modification was conducted by putting them into the ethanol solution of 20 mmol/L PFDTs for 12 h.

### 1.3 Characterization

The morphologies of prepared surfaces were observed by environmental scanning electron microscopy (SEM, FEI Quanta200 FEG, America). X-ray photoelectron spectroscopy (XPS) analyses of samples were conducted on a spectrometer with Mg K $\alpha$  X-ray source. The CA and RA were measured with a water droplet (4  $\mu\text{L}$ ) by a contact angle meter (OCA20, Dataphysics GmbH, Germany). The final angle values were

averaged from five different measurements for each sample. The anticorrosion behaviors in 3.5 wt% NaCl solution were tested by the electrochemical impedance spectroscopy (EIS) and potentiodynamic polarization curves at room temperature using an electrochemical workstation (CHI660D, Chen Hua Instrument Co., Ltd, Shanghai, China). A standard three-electrode system was used in the test and the sample with an exposed area of 1  $\text{cm}^2$  was used as the working electrode. The polarization curve was recorded by the linear sweep voltammetry from  $-1800$  mV to  $-200$  mV with a scanning rate of 1 mV/s. The EIS was tested between 10 mHz and 100 kHz with a sine wave amplitude of 10 mV. Prior to electrochemical testing, all working electrodes were immersed in the electrolyte for 30 min to reach a steady state.

## 2 Results and Discussion

### 2.1 Fabrication of superhydrophobic surfaces

Fig.1 shows the microcosmic morphologies of the Al alloy substrate and machined sample. As seen in Fig.1a, a relatively smooth surface with some abrasive grooves is obtained on the metallic substrate. After the WEDM process, Al alloy surface is covered with microscale wrinkles with a size range of 15~25  $\mu\text{m}$  (Fig.1b). Furthermore, the magnified SEM image in Fig.1c reveals the nanostructures. Clearly, many nanoscale craters are observed on wrinkled surface. The formation of wrinkles and craters can be attributed to the local fusion and evaporation of the Al alloy surface induced by the applied charges, as shown in Fig.1d. The local defects and weak phases on the metallic surface may develop into the initial points for forming rough structures. Furthermore, the exertion of continuous energy leads to a constant increase in temperature for melting and vaporizing samples. As a result, the rough structures gradually evolve into wrinkles and craters on Al alloy surfaces.

Generally, PFDTs modification is an effective method to fabricate the low-surface-energy surface<sup>[18]</sup>. The wettability of the Al alloy substrate and the machined sample after modification is shown in Fig.2. Clearly, a hydrophobic CA of 103.6° is observed for the modified substrate (Fig.2a). In contrast, for the modified machined surface, a superhydrophobic CA of 152.7° (>150°) is found (Fig.2c). Furthermore, the RA test is also an indispensable condition for assessing the wettability. As seen in Fig.2b, a droplet remains adhered to the modified substrate even when tilted to 90°, suggesting a strong adhesion. However, a tiny RA of 7.1° (<10°) is achieved for the modified machined surface, indicating a superior superhydrophobicity. Hence, the wettabilities on Al alloy surfaces can be manipulated from hydrophilic to superhydrophobic by preparing micro-nano wrinkles and craters. In addition, the Wenzel wetting model<sup>[19]</sup> clearly states that hierarchical rough structures have positive effects on surface wettability. Just owing to the increased roughness of micro-nano structures, the machined surface is propitious to

**Table 1 Chemical composition of 5A05 Al alloy (wt%)**

Mg	Mn	Fe	Si	Zn	Cu	Al
5.50	0.60	0.50	0.50	0.20	0.10	92.60

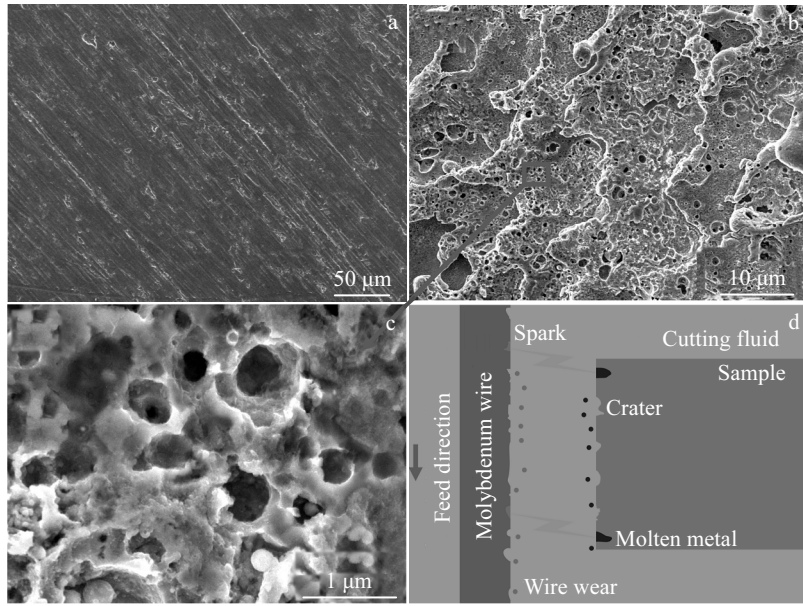


Fig.1 SEM images of Al alloy substrate (a), and machined surface (b, c), referring to the WEDM processing principle (d)

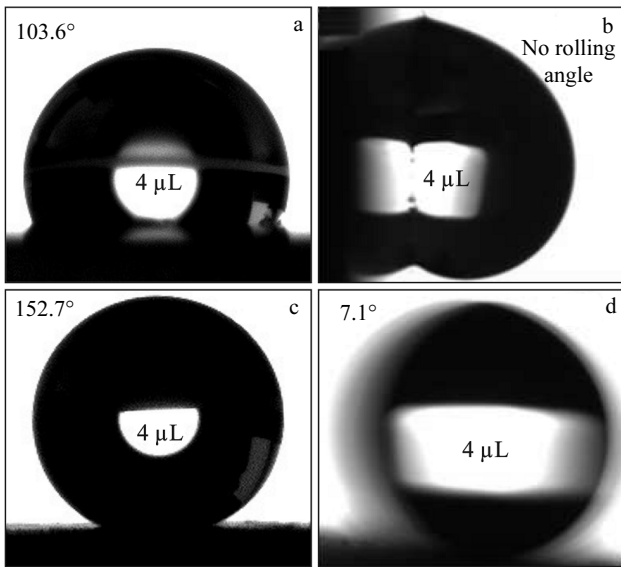


Fig.2 Wettabilities of modified Al alloy substrate (a, b) and modified machined sample (c, d)

obtain superhydrophobicity compared with the smooth counterpart.

Fig.3 shows the XPS spectra of the machined Al alloys samples before and after modification. Obviously, new element peaks of Si 2s and F 1s are observed on the modified surface compared with the untreated one. It implies that the PFDTs layer with Si and F elements has been successfully incorporated on the machined surface. Generally, F element has a strong electrophilic ability, which can endow C-F bond

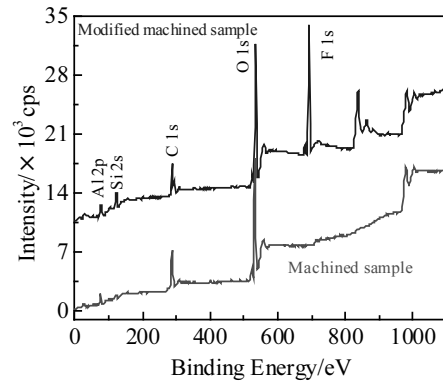


Fig.3 XPS spectra of the machined Al alloy surfaces before and after modification

with strong chemical inertness<sup>[20]</sup>. Consequently, the PFDTs layer on surface has been prepared with low surface energy, which is conducive to repelling water. For this reason, PFDTs modification can endow the machined Al alloy surface with excellent superhydrophobicity.

To further test the water adhesion of the modified machined surface, a bouncing experiment for a water droplet (4 μL) was conducted and the results are shown in Fig.4. In the whole test, the droplet is freely released and the snapshots are recorded at 400 fps using a high-speed camera. The initial state shows the distance between the droplet and the sample. In this situation, the droplet displays a natural appearance due to the gravity. As the test time is extended to 2.5 ms, the droplet just touches the sample. At 5.0 ms, a completely squeezed droplet is observed and then it starts to rebound. After that, the droplet keeps

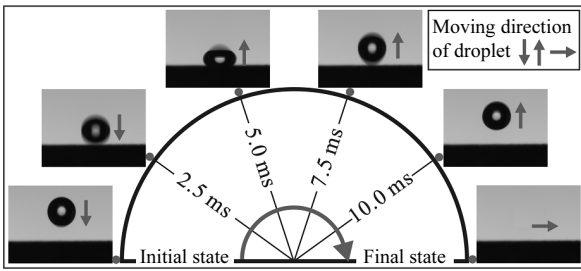


Fig.4 Snapshots of a droplet impacting the superhydrophobic surface

bouncing back and forth for many times before rolling off the sample in the final state. Note that there is no any residual water on the as-prepared surface. This test indicates that the water adhesion and drag resistance of the superhydrophobic sample are negligible.

**2.2 Corrosion resistance of Al alloy surfaces**

Fig.5 shows the anticorrosion behaviors of Al alloy samples with various processes tested by potentiodynamic polarization curves in 3.5 wt% NaCl solution at room temperature. Generally, a surface with low corrosion current density ( $I$ ) and positive-shifting corrosion potential ( $E$ ) has superior corrosion resistance<sup>[21]</sup>. After fitting with the Tafel extrapolation method, the corrosion current densities of the substrate, modified

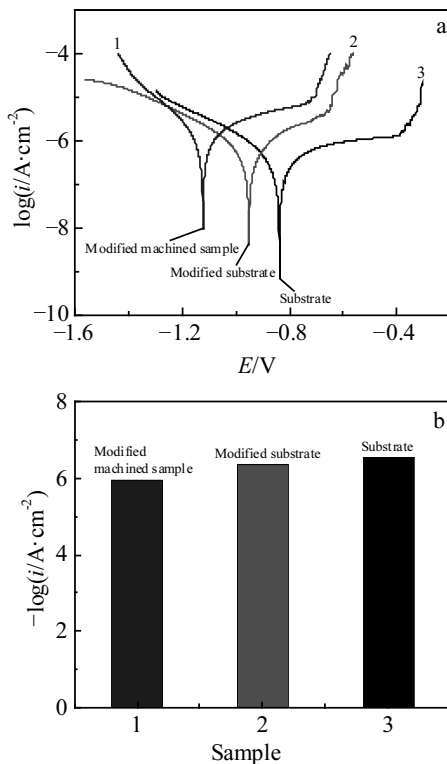


Fig.5 Potentiodynamic polarization curves (a) and corrosion current densities (b) of Al alloy samples with various processes

substrate and modified machined samples are 1.139, 0.441 and 0.283  $\mu\text{A}/\text{cm}^2$ , respectively. Meanwhile, the corrosion potentials of the three samples shift positively from  $-1.124$ ,  $-0.952$  to  $-0.838$  V. After comparison, Al alloy substrate shows the worst corrosion resistance. This is attributed to the abundant active chlorine ions in seawater, which can corrode substrates and lead to penetrating and pitting failures, as shown in Fig.6a. However, the anticorrosion behavior of Al alloy substrate has been greatly improved after the PFDTs modification. This is ascribed to the modified PFDTs film, which can prevent the seawater penetration by impeding the interfacial interactions between the substrate and corrosive ions, as exhibited in Fig.6b. Furthermore, the WEDM processed surface exhibits the best corrosion resistance compared with the other two samples. As mentioned above, the hierarchical micro-nano structures play an important role in developing the superhydrophobicity, which can also increase the chance for trapping air, as seen in Fig.6c. Most of all, the trapped air can act as a dielectric for parallel plate capacitors, which can keep electrons from transferring between the electrolyte and the fabricated surface. Under the combined action of PFDTs film, the superhydrophobic surface achieves the best corrosion resistance.

In order to determine the corrosion rates of various samples, the corrosion inhibition efficiency ( $E_i$ ) is computed in Eq.(1)<sup>[22]</sup>:

$$E_i = \frac{I_1 - I_2}{I_1} \quad (1)$$

where  $I_1$  and  $I_2$  refer to the corrosion current densities of sample 1 and sample 2, respectively. This equation indicates that  $E_i$  of the modified machined sample compared with the Al alloy substrate and modified substrate are 75.15% and 35.83%, respectively. Additionally, after comparing the corrosion current densities, the modified machined sample has better anticorrosion ability than other works with various processes, as shown in Table 2.

Furthermore, the corrosion resistance can also be characterized by EIS measurements. Fig.7 shows the resultant

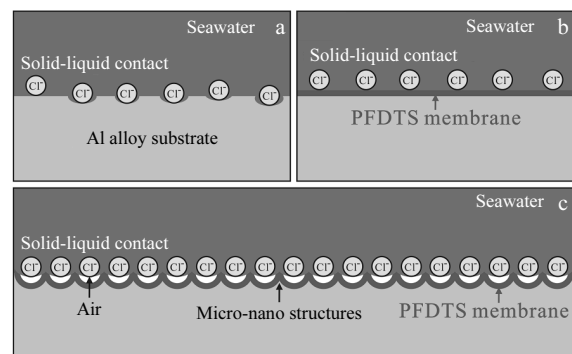


Fig.6 Anticorrosion mechanisms of Al alloy substrate (a), modified substrate (b), and modified machined sample (c)

**Table 2** Anticorrosion behaviors of superhydrophobic Al alloys with various processes in different works

Reference	Process	$i/\mu\text{A}\cdot\text{cm}^{-2}$
[23]	NaOH etching	0.90
[24]	Immersion and then ultrasound treating	1.25
[25]	NaOH/CuCl <sub>2</sub> etching and then annealing	1.84
[26]	NaOCl etching and then passivating	2.95
[27]	Boiling water etching	11.60
This work	WEDM process	0.28

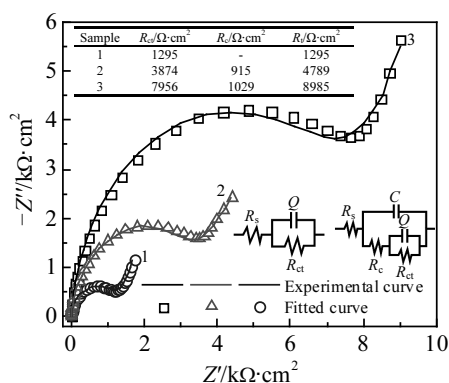


Fig.7 Experimental and fitted EIS plots of Al alloy substrate (1), modified substrate (2), and modified machined sample (3)

Nyquist plots of the Al alloy substrate, modified substrate and modified machined sample, where the semicircle refers to the capacitance arc, which is used for assessing the polarization resistance. A large polarization resistance means a better impeditive ability for transferring electrons<sup>[28]</sup>. Hence, a large semicircle diameter indicates a weak ability of anions to transfer between the corrosive medium and sample, which also suggests a superior anticorrosion ability. It can be clearly seen from Fig.7 that the semicircle diameter as well as the anticorrosion ability of the modified machined sample is the largest, followed by the modified substrate and then the substrate. The same tendency of anticorrosion abilities exhibited in polarization curves is also observed in EIS measurements. In brief, the corrosion resistance of 5A05 Al alloys is greatly improved with the WEDM process and PFDTs modification. To obtain the electrochemical data for above samples, EIS curves are also fitted using the ZSimDemo software in Fig.7. The experimental curve for Al alloy substrate is specifically well fitted with the circuit pattern  $R_s(QR_{ct})$ , where  $R_s$ ,  $R_{ct}$  and  $Q$  refer to solution resistance, charge-transfer resistance and double-layer capacitance, respectively. The corrosion curves for modified samples are well fitted with the pattern  $R_s\{C[R_c(QR_{ct})]\}$ , where  $C$  and  $R_c$  denote the capacitance and resistance of the modified films, respectively. Meanwhile, the fitted curves can well match the experimental results, suggesting a reasonable simulation for EIS curves in this work. Furthermore, the corresponding fitted data is also displayed in Fig.7. Clearly, an

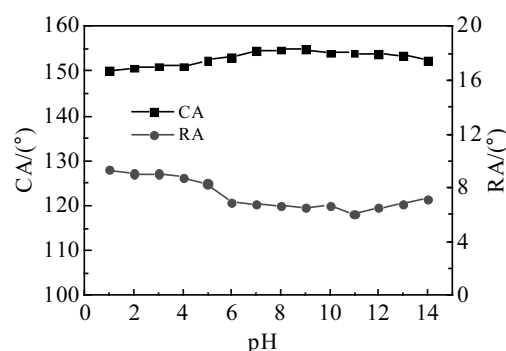


Fig.8 Relationship between pH values and wettabilities of the superhydrophobic surface

increasing polarization resistance ( $R_t = R_{ct} + R_c$ ) for Al alloy substrate, modified substrate and modified machined sample is attained, indicating a gradually enhanced charge-transfer resistance and corrosion resistance, which is in good agreement with the experimental.

To test and verify the chemical stability of the superhydrophobic sample, Fig.8 shows the relationship between pH values and wettabilities of the as-prepared surface. Clearly, there is no obvious fluctuation in CA and RA values when the pH varying from 1 to 14. It suggests that the corrosive mediums have little effect on the superhydrophobicity, which is consistent with the previous work<sup>[29]</sup>. Actually, the superhydrophobicity of Al alloy sample is mainly due to its hierarchical micro-nano structures and PFDTs modifiers. Hence, the chemical stability of the superhydrophobic 5A05 Al alloy has been achieved to expand its potential applications as an engineering material in corrosive environments.

### 3 Conclusions

- 1) The superhydrophobic microscale wrinkles covered with nanoscale craters can be fabricated on 5A05 Al alloy surface by a one-step wire-cut electrical discharge machining process.
- 2) After the PFDTs modification, the as-prepared micro-nano structures exhibits excellent superhydrophobicity with a water contact angle of 152.7° and a rolling angle of 7.1°. Such a surface is also found with extremely weak water adhesion and drag resistance.
- 3) The superhydrophobic Al alloy surface has excellent chemical stability. Owing to the composite solid-air-liquid interfaces, it can also resist the seawater corrosion by reducing the interfacial interactions with corrosive ions.

### References

- 1 Yang Q Y, Liu W Y, Zhang Z Q et al. *Rare Metal Materials and Engineering*[J], 2018, 47(2): 409
- 2 Liu F C, Xiong Q P, Liu Q et al. *Rare Metal Materials and Engineering*[J], 2015, 44(7): 1786
- 3 Xie H J, Cheng Y L, Li S X et al. *Transactions of Nonferrous*

- Metals Society of China*[J], 2017, 27(2): 336
- 4 Bokati K S, Dehghanian C. *Journal of Environmental Chemical Engineering*[J], 2018, 6(2): 1613
- 5 Xu X J, Zhu J X, Guo Y F. *Rare Metal Materials and Engineering*[J], 2017, 46(10): 2981
- 6 Wang H, Ning C, Huang Y et al. *Optics & Lasers in Engineering*[J], 2017, 90: 179
- 7 Vitry V, Sens A, Kanta A F et al. *Surface & Coatings Technology*[J], 2012, 206(16): 3421
- 8 Hubadillah S K, Kumar P, Othman M H D et al. *RSC Advances*[J], 2018, 8(6): 2986
- 9 Kondo R, Nakajima D, Kikuchi T et al. *Journal of Alloys & Compounds*[J], 2017, 725: 379
- 10 Lee J W, Hwang W. *Materials Letters*[J], 2016, 168: 83
- 11 Razavi S M R, Masoomi M, Bagheri R. *Colloids & Surfaces A Physicochemical & Engineering Aspects*[J], 2018, 541: 108
- 12 Feng L, Zhang H, Wang Z et al. *Colloids & Surfaces A Physicochemical & Engineering Aspects*[J], 2014, 441(3): 319
- 13 Wang Y, Zhang X W, Zhou H F et al. *Chemical Research in Chinese Universities*[J], 2016, 32(2): 155
- 14 Feng L, Yan Z, Shi X et al. *Applied Physics A*[J], 2018, 124(2): 142
- 15 Zhang K, Wu J, Chu P et al. *International Journal of Electrochemical Science*[J], 2015, 10(8): 6257
- 16 Xia B B, Liu H T, Fan Y N et al. *Materials & Design*[J], 2017, 135: 51
- 17 Liu Y, Li X, Yan Y et al. *Surface & Coatings Technology*[J], 2017, 331: 7
- 18 Bahrami H R T, Ahmadi B, Saffari H. *Materials Letters*[J], 2017, 189: 62
- 19 Li X W, Zhang Q X, Guo Z et al. *Applied Surface Science*[J], 2015, 342: 76
- 20 Li X W, Zhang Q X, Guo Z et al. *RSC Advances*[J], 2015, 5(38): 29 639
- 21 Chen Y, Zhang J, Dai N et al. *Electrochimica Acta*[J], 2017, 232: 89
- 22 Chen Z, Shuai M, Wang L. *Journal of Solid State Electrochemistry*[J], 2013, 17(10): 2661
- 23 Wankhede R G, Morey S, Khanna A S et al. *Applied Surface Science*[J], 2013, 283(20): 1051
- 24 Rezayi T, Entezari M H. *Journal of Colloid & Interface Science*[J], 2016, 463: 37
- 25 Cheng Y, Lu S, Xu W. *New Journal of Chemistry*[J], 2015, 39(8): 6602
- 26 Lv D, Ou J, Xue M et al. *Applied Surface Science*[J], 2015, 333: 163
- 27 Feng L, Yan Z, Qiang X et al. *Surface & Interface Analysis*[J], 2015, 47(4): 506
- 28 Jia Z, Duan X G, Qin P et al. *Advanced Functional Materials*[J], 2017, 27(38): 1 702 258
- 29 Zhang Q X, Chen Y X, Guo Z et al. *ACS Applied Materials & Interfaces*[J], 2013, 5(21): 10 633

## 5A05 铝合金表面超疏水结构的制备及耐腐蚀性

张传伟<sup>1</sup>, 李雪伍<sup>1</sup>, 石甜<sup>1</sup>, 张来昌<sup>2</sup>

(1. 西安科技大学, 陕西 西安 710054)

(2. 埃迪斯科文大学, 西澳大利亚州 珀斯 6027, 澳大利亚)

**摘要:** 以 5A05 铝合金为研究对象, 提出一种简单的低成本超疏水结构制备方法, 实现了超疏水/耐腐蚀表面的可控构筑。采用电火花线切割技术, 对基材表面进行微米级褶皱与纳米级凹坑结构的一步高效制备, 并对结构改性后的润湿性和耐腐蚀性进行系统测量与表征。结果表明, 改性后的表面水滴静态接触角高达 152.7°, 滚动角仅为 7.1°, 表现出优异的超疏水性。进一步的电化学测试结果表明, 超疏水表面通过改变界面作用行为, 减弱了固-气-液复合接触界面间腐蚀介质的作用行为与过程, 对表面耐腐蚀性产生决定性影响, 明显提高了材料的抗腐蚀性。

**关键词:** 铝合金; 微纳结构; 超疏水; 耐腐蚀

作者简介: 张传伟, 男, 1974 年生, 博士, 教授, 西安科技大学机械工程学院, 陕西 西安 710054, 电话: 029-85583159, E-mail: zhangcw@xust.edu.cn